Modern Physics Letters A

THE BLAST EXPERIMENT: POLARIZED ELECTRON SCATTERING FROM HYDROGEN AND DEUTERIUM

R. ALARCON

Department of Physics, Arizona State University
Tempe, AZ 85287-1504, USA
ralarcon@asu.edu

THE BLAST COLLABORATION

Received (Day Month Year)
Revised (Day Month Year)

At the MIT-Bates Linear Accelerator Center, the nucleon form factors have been measured by scattering polarized electrons from vector-polarized hydrogen and deuterium. The experiment used the longitudinally polarized electron beam stored in the MIT-Bates South Hall Ring along with an isotopically pure, highly vector-polarized internal atomic hydrogen and deuterium target provided by an atomic beam source. The measurements were carried out with the symmetric Bates Large Acceptance Spectrometer Toroid (BLAST). Results are presented for the proton form factor ratio, $\mu_p G_E^p/G_M^p$, and for the charge form factor of the neutron, G_E^n. Both results are more precise than previous data in the corresponding Q^2 ranges.

Keywords: Polarized electron scattering; nucleon form factors.

PACS Nos.: 25.30.-c, 25.30.Rw, 29.25.-t, 29.30.-h.

1. The BLAST Experiment

The BLAST experiment was designed to measure spin-dependent electron scattering at intermediate energies from polarized targets in the elastic, quasielastic and resonance region. Based on the internal target technique BLAST optimizes the use of a longitudinally polarized electron beam stored in the South Hall Ring of the MIT-Bates Linear Accelerator Center, in combination with an isotopically pure, highly-polarized internal target of hydrogen or deuterium. In case of deuterium the target was both vector and tensor polarized. The polarized target was provided by an atomic beam source (ABS) [1].

At Bates beam currents of up to 225 mA were stored in the ring at 65% polarization and beam lifetimes of 20-30 minutes. The electron beam energy was 850 MeV and the relatively thin target in combination with the high beam intensity yielded a luminosity of about $5{\times}10^{31}/(\mathrm{cm}^2\,\mathrm{s})$ at an average current of 175 mA. The Bates storage ring included a Compton polarimeter to monitor the longitudinal beam polarization in real time and without affecting the beam. The electron spin precession

was compensated using a spin rotator (Siberian snake) in the ring section opposite to BLAST. The helicity of the beam was flipped once before every ring fill.

The BLAST detector is schematically shown in Fig. 1. It was built as a toroidal

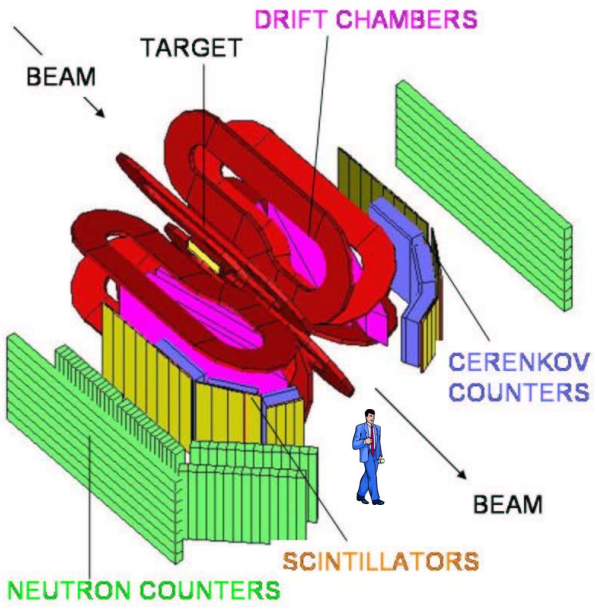

Fig. 1. Schematic, isometric view of the BLAST detector showing the main detector elements.

spectrometer consisting of eight normal-conducting copper coils producing a maximum field of 3800 G. The two in-plane sectors opposing each other were symmetrically equipped with drift chambers for the reconstruction of charged tracks, aerogel-Cerenkov detectors for e/π discrimination and 1" thick plastic scintillators for timing, triggering and particle identification. The angular acceptance covered scattering angles between 20°and 80°and ±15°out of plane. The symmetric detector core was surrounded by thick large-area walls of plastic scintillators for the detection of neutrons using the time-of-flight method.

The BLAST experiment made use of elastic *ep*-scattering of polarized electrons from polarized hydrogen to access the proton form factors, quasielastic $(\vec{e}, e'n)$ scat-

tering from vector-polarized deuterium to get at the charge form factor of the neutron, inclusive $(\vec{e}, e')$ scattering from vector-polarized deuterium for the magnetic form factor of the neutron, and elastic ed scattering to measure tensor analyzing powers to help separate the deuteron form factors. In what follows results are presented for the form factors of the proton and the charge form factor of the neutron.

2. Nucleon Structure

The electromagnetic structure of the nucleon is traditionally described in terms of two form factors and it has been extensively studied by the scattering of electrons on nucleons. Experiments on electron-proton scattering have yielded abundant information on the magnetic G_M^p and charge G_E^p form factors of the proton in the range of momentum transfers squared, Q^2, up to about 30 $(\mathrm{GeV/c})^2$. The information on the neutron form factors comes almost entirely from the scattering of electrons on deuterons or ^3He nuclei, and it is much less definite than that on the proton. The difficulty is due mainly to final state interactions, mesonic currents, and the fact that the form factors of nucleons inside the deuteron or ^3He may differ from those of free particles.

In recent years the advent of polarized beams, targets, and polarimetry have made possible new classes of experiments aimed at extracting the nucleon form factors utilizing spin degrees of freedom. The general form for the differential cross section in the exclusive scattering of longitudinally polarized electrons from a polarized target is given by [2]

$$\frac{d\sigma}{de' d\Omega'_e d\Omega_N} = \Sigma + h\Delta \tag{1}$$

where h is the helicity of the incident electron, and Σ and Δ are the helicity-sum and helicity-difference cross sections, respectively. The Σ and Δ cross sections for the case of elastic scattering from a polarized nucleon can be written as

$$\Sigma = c(\rho_L G_E^2 + \rho_T \frac{q^2}{2M^2} G_M^2) \tag{2}$$

and

$$\Delta = -c(\rho'_{LT} \frac{q}{2^{3/2}M} G_E G_M P_x + \rho'_T \frac{q^2}{2M^2} G_M^2 P_z) \tag{3}$$

where c is a kinematical factor, the ρ's are the virtual photon densities, and P_j indicates the polarization of the nucleon along each of the three coordinate axes, of which the z-axis has been chosen parallel to the momentum transfer $\vec{q}$. The terms containing $G_E G_M$ and G_M^2 can be completely isolated by tuning the target spin polarization. Experimentally one measures spin asymmetries defined as

$$A_{exp} = p_e p_T \frac{\Delta}{\Sigma} \tag{4}$$

where p_e and p_T are the electron beam and target polarization, respectively. To separate both terms of the Δ cross section the target spin is oriented perpendicular (parallel) to the direction of $\vec{q}$ (i.e., selecting P_x (P_z)).

2.1. *Proton Electric to Magnetic Form Factor Ratio*

The polarized hydrogen data were divided into eight Q^2 bins and the yield distributions were in good agreement with results from a Monte Carlo simulation, including all detector efficiencies measured from the data. The BLAST detector configuration was symmetric about the incident electron beam and the target polarization angle was oriented $\sim 45^\circ$ to the left of the beam. Two independent asymmetries of electrons scattered into the beam-left and beam-right sectors, respectively, were measured simultaneously. The ratio G_E^p/G_M^p could then be determined, independent of p_e and p_T, from the ratio of these experimental asymmetries measured at the same Q^2 value but corresponding to different spin orientations [3].

Results for G_E^p/G_M^p are shown in Fig. 2 [4] together with published recoil polar-

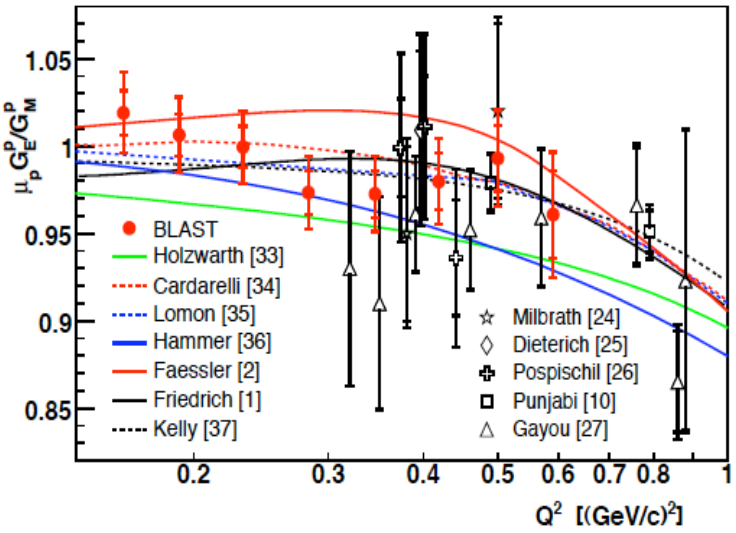

Fig. 2. Results of $\mu_p G_E^p/G_M^p$ shown with the world polarized data as a function of Q^2 up to 1 (GeV/c)^2.

ization data [5,6,7,8,9,10,11], together with a few selected models: a soliton model [12], an extended vector meson dominance model [13], an updated dispersion model [14], a relativistic constituent quark model (CQM) with SU(6) symmetry breaking and a constituent quark form factor [15], and a Lorentz covariant chiral quark model [16].

2.2. *Neutron Electric Form Factor*

With BLAST measurements of G_E^n were carried out by means of $(e, e'n)$ quasi-elastic scattering using polarized electrons and a vector-polarized deuterium target. The experimental double spin asymmetry was formed from the measured $(e, e'n)$-yields in each beam-target spin state combination, properly normalized to the collected deadtime-corrected beam charge. For five bins in Q^2, the experimental asymmetry as a function of missing momentum was compared with the full BLAST Monte-carlo result based on deuteron electrodisintegration cross section calculations by H. Arenhövel[17] with consistent inclusion of reaction mechanism and deuteron structure effects. The electric form factor of the neutron was varied as an input parameter to the Montecarlo simulation and its measured value was extracted by a χ^2 minimization for each Q^2 bin [18,19].

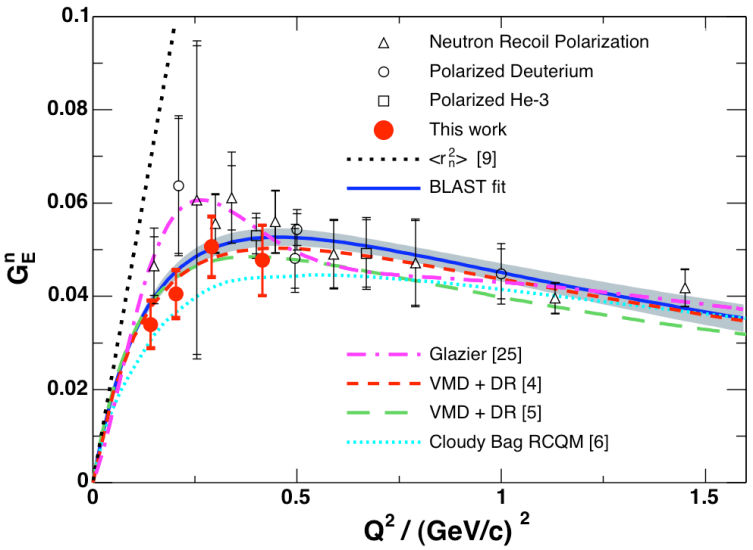

Fig. 3. Electric form factor of the neutron from polarization experiments [20] along with results from BLAST. The curves are the recent parameterizations by Friedrich and Walcher [21], dispersion analyses (VMD+DR) [13,23], and a meson-cloud model. [24]

The results [22] are displayed in Fig. 3 along with the world's data on the neutron charge form factor G_E^n from double polarization experiments[20]. The new data from BLAST do not show a pronounced bump structure at low Q^2as previously suggested

(see Fig. 3). The BLAST data are in excellent agreement with the dispersion analysis and also agree well with the meson-cloud model .

3. Summary

Results for the electromagnetic form factors of the nucleon have been obtained with the BLAST experiment. The technique utilized a combination of polarized electron beam, polarized internal gas targets, and a large acceptance detector. These new measurements cover a range of four-momentum transfer Q^2 between 0.12 and 0.70 $(GeV/c)^2$. The proton electric to magnetic form factor ratio was measured by elastic *ep*-scattering of polarized electrons from polarized hydrogen. The neutron electric form factor was extracted from measurements of quasielastic $(\vec{e}, e'n)$ scattering from vector-polarized deuterium. Both results are more precise than previous data in the corresponding Q^2 ranges.

Acknowledgments

This work was supported in part by grants PHY-0354878 and PHY-0652393 of the US National Science Foundation.

References

1. D. Cheever *et al.*, Nucl. Instr. Meth. **A556**, 410 (2006); L.D. van Buuren *et al.*, Nucl. Instr. Meth. **A474**, 209 (2001).
2. T.W. Donnelly and A.S. Raskin, Ann. Phys. **169**, 247 (1986).
3. C.B. Crawford, Ph.D. thesis, Massachusetts Institute of Technology (2005).
4. C.B. Crawford, *et al.*, Phys. Rev. Lett. **98**, 052301 (2007).
5. M. Jones *et al.*, Phys. Rev. Lett. **84**, 1398 (2000).
6. O. Gayou *et al.*, Phys. Rev. Lett. **88**, 092301 (2002).
7. V. Punjabi *et al.*, Phys. Rev. **C71**, 055202 (2005).
8. O. Gayou *et al.*, Phys. Rev. **C64**, 038202 (2001).
9. S. Dieterich *et al.*, Phys. Lett. **B500**, 47 (2001).
10. T. Pospischil *et al.*, Eur. Phys. J. **A12**, 125 (2001)
11. B. Milbrath *et al.*, Phys. Rev. Lett. **80**, 452 (1998), and **82**, 2221(E) (1999).
12. G. Holzwarth, Z. Phys. **A356** (1996) 339.
13. E.L. Lomon, Phys. Rev. **C66**, 045501 (2002).
14. H.-W. Hammer and Ulf-G. Meissner, Eur. Phys. J. **A20**, 469 (2004).
15. F. Cardarelli and S. Simula, Phys. Rev. **C62**, 065201 (2000).
16. A. Faessler, T. Gutsche, V. Lyubovitskij, K. Pumsaard, Phys. Rev. **D73**, 114021 (2006).
17. H. Arenhövel, W. Leidemann, and E.L. Tomusiak, *Eur. Phys. J.* **A23**, 147 (2005).
18. V. Ziskin, Ph.D. Thesis, Massachusetts Institute of Technology (2005).
19. E. Geis, Ph.D. Thesis, Arizona State University (2007).
20. D.I. Glazier *et al.*, *Eur. Phys. J.* **A24**, 101 (2005) and references therein.
21. J. Friedrich and T. Walcher, Eur. Phys. J. **A17**, 607 (2003).
22. E. Geis, M. Kohl, V. Ziskin, *et al.*, Phys. Rev. Lett. **101**, 042501 (2008).
23. M. Belushkin, H. Hammer, and U. Meissner, Phys. Rev. **C75**, 035202 (2007).
24. G. A. Miller, Phys. Rev. **C 66**, 032201(R) (2002).